Internal Gravity (Buoyancy) Waves

(Holton 7.4)

- Wave parameters
- Pure internal gravity waves (no topography)
  - Parcel oscillations
  - Linearized equations
  - Solutions & wave parameters (dispersion relationship)
  - Group velocity

A wave with wavelength = 2π traveling at speed c in the x-direction

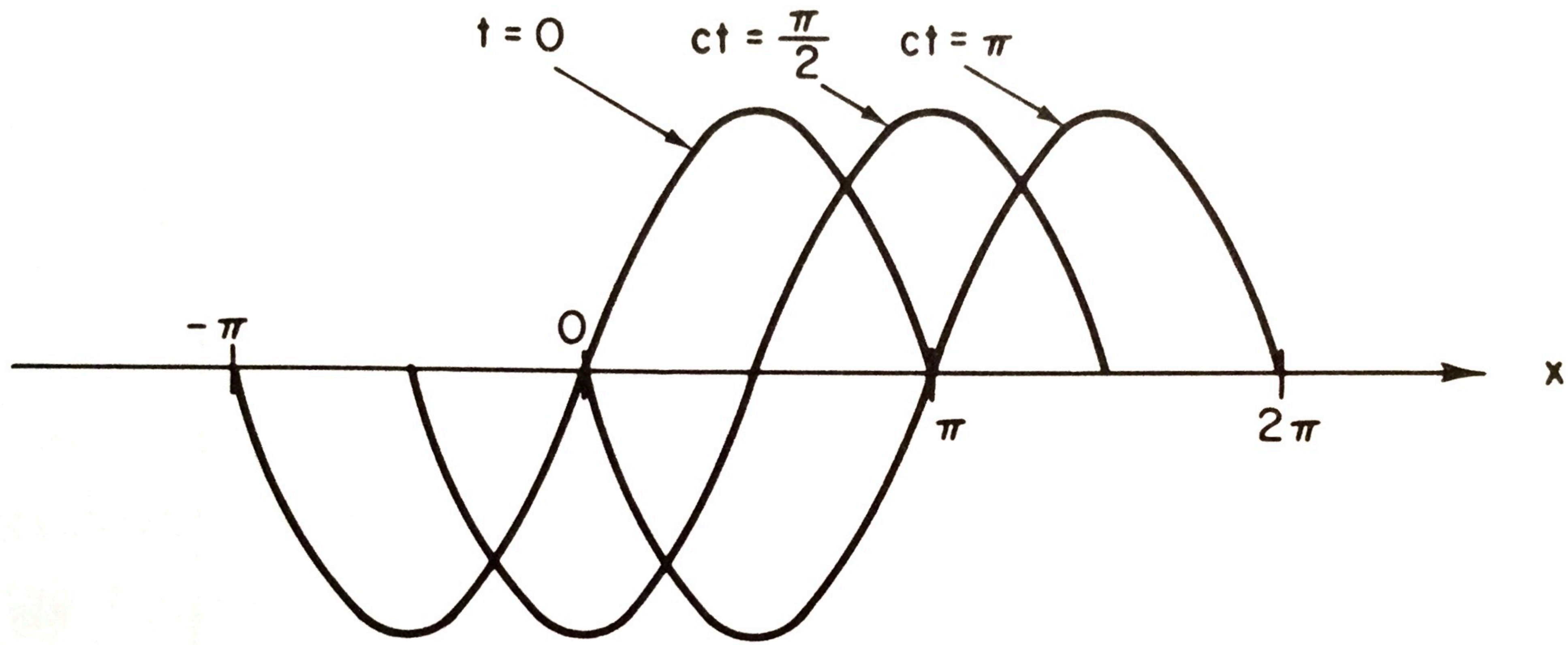

Fig. 7.2 A sinusoidal wave traveling in the positive x direction at speed c. (Wave number is assumed to be unity.)

Wave Parameters

For a function having a wave structure in the x and z directions (Figure 6.4), we modify (6.2) to include the second direction such that it becomes

$$f = A\cos(kx + mz - \omega t) \tag{6.3}$$

where $m = 2\pi/\lambda_z$ and λ_z is the vertical wavelength. For notational convenience and to allow for cosine as well as sine solutions, we shall often express our assumed wave solutions in the form

$$f = \Re\left\{Ae^{i(kx+mz-\omega t)}\right\} \tag{6.4}$$

where A is now a complex amplitude (i.e., $A = A_r + iA_i$), $e^{i(kx+mz-\omega t)}$ expands to $\cos(kx + mz - \omega t) + i\sin(kx + mz - \omega t)$, and the $\Re$ operator indicates that we retain only the real part of the quantity in brackets.

At any particular time, the quantity $kx + mz - \omega t$ is described as the *phase* of the wave, and lines of constant phase are called *wavefronts*, which are perpendicular to the *wave vector* (also sometimes called the *wavenumber vector*) $\boldsymbol{\kappa} = k\mathbf{i} + m\mathbf{k}$. We can write (6.3) using the wave vector and a position vector, $\mathbf{r} = x\mathbf{i} + z\mathbf{k}$, to obtain

$$f = A\cos(\boldsymbol{\kappa}\cdot\mathbf{r} - \omega t)\,. \tag{6.5}$$

$k = 2\pi/\lambda_x$: horizontal wavenumber
$m = 2\pi/\lambda_z$: vertical wavenumber

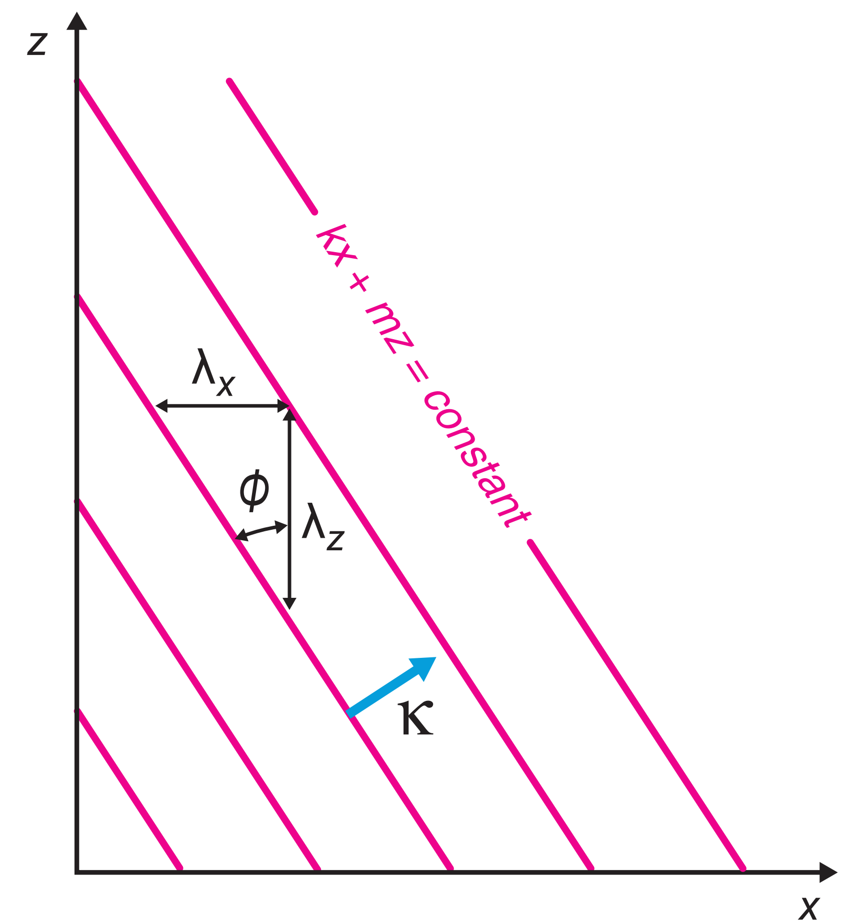

Figure 6.4 Basic wave properties. Lines indicate constant phase for a plane wave; λ_x (k) and λ_z (m) are the wavelengths (wavenumbers) in the x and z directions, respectively, ϕ is the angle between the phase lines and the vertical, and $\boldsymbol{\kappa}$ is the wave vector.

Parcel Oscillations

(Thermo Notes, Section 7.2

$$\frac{dw}{dt} = g\frac{T - \bar{T}}{\bar{T}}.$$

Let $z = 0$ denote the parcel's equilibrium location. Then at $z = 0$, $T = \bar{T}$, and $dw/dt = 0$.

Assume that the temperature in the environment varies linearly with height. Then the temperature at any height z in the environment is

$$\bar{T}(z) = \bar{T}(0) - \gamma z,$$

where $\gamma = -d\bar{T}/dz$ is the *environmental lapse rate.* Similarly, the parcel temperature at any height z is

$$T(z) = T(0) - \Gamma_d z = \bar{T}(0) - \Gamma z,$$

where $\Gamma_= - dT/dz$ is the *parcel lapse rate*

$$\frac{dw}{dt} = g\frac{T - \bar{T}}{\bar{T}}.$$

When these expressions are substituted in Eq. (41), we obtain

$$\frac{dw}{dt} = \frac{g}{\bar{T}(0) - \gamma z}(\gamma - \Gamma)z \approx \frac{g}{\bar{T}(0)}(\gamma - \Gamma)z = bz. \tag{42}$$

$$\frac{dw}{dt} = g\frac{T - \bar{T}}{\bar{T}}.$$

When these expressions are substituted in Eq. (41), we obtain

$$\frac{dw}{dt} = \frac{g}{\bar{T}(0) - \gamma z}(\gamma - \Gamma)z \approx \frac{g}{\bar{T}(0)}(\gamma - \Gamma)z = bz. \tag{42}$$

Eq. (42) describes how w changes with time. By definition,

$$\frac{dz}{dt} = w. \tag{43}$$

Eqs. (42) and (43) are coupled linear differential equations which are easy to solve analytically for $z(t)$.

They can also be combined into a single second-order differential equation:

$$\frac{d^2z}{dt^2} = bz.$$

$$b = \frac{g}{\bar{T}(0)}(d\bar{T}/dz - \Gamma) = -\frac{g}{\bar{T}(0)}\frac{d\bar{\theta}}{dz} \equiv -N^2$$

$$N^2 \equiv \frac{g}{\theta_0}\frac{d\theta}{dz}$$

Parcel Oscillations

Parcel is displaced a distance δs along line tilted at angle α.

Vertical displacement is $\delta z = \delta s\ \cos\alpha$.

Vertical buoyancy force is $-N^2\delta z$, where $N^2 \equiv \frac{g}{\theta}\frac{d\theta}{dz}$.

Component of buoyancy force parallel to tilted path is

$$-N^2\delta z\cos\alpha = N^2(\delta s\ \cos\alpha)\cos\alpha = -(N\cos\alpha)^2\delta s$$

Momentum equation for parcel is

$$\frac{d^2(\delta s)}{dt^2} = -(N\cos\alpha)^2\delta s$$

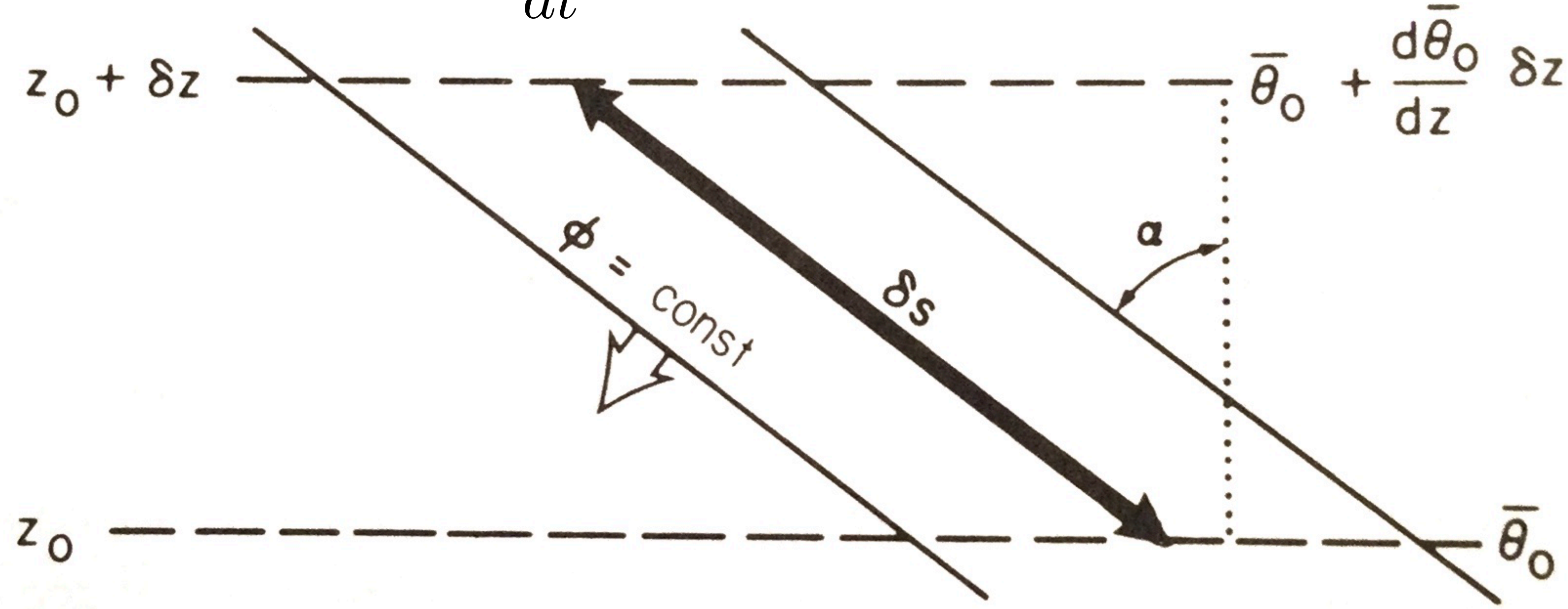

Fig. 7.8 Parcel oscillation path (heavy arrow) for pure gravity waves with phase lines tilted at an angle α to the vertical.

Linearized Equations

For two-dimensional motion:

$$\frac{\partial u}{\partial t} + u\frac{\partial u}{\partial x} + w\frac{\partial u}{\partial z} = -\frac{1}{\overline{\rho}}\frac{\partial p'}{\partial x}$$

$$\frac{\partial w}{\partial t} + u\frac{\partial w}{\partial x} + w\frac{\partial w}{\partial z} = -\frac{1}{\overline{\rho}}\frac{\partial p'}{\partial z} + g\frac{\theta'}{\overline{\theta}}$$

$$\frac{\partial u}{\partial x} + \frac{\partial w}{\partial z} = 0$$

$$\frac{\partial \theta}{\partial t} + u\frac{\partial \theta}{\partial x} + w\frac{\partial \theta}{\partial z} = 0$$

Linearize:

$$u = \bar{u} + u'$$
$$w = w'$$
$$p = \bar{p}(z) + p'$$
$$\theta = \bar{\theta} + \theta'$$

Linearized Equations

$$\left(\frac{\partial}{\partial t}+\bar{u}\frac{\partial}{\partial x}\right)u'+\frac{1}{\rho_0}\frac{\partial p'}{\partial x}=0$$

$$\left(\frac{\partial}{\partial t}+\bar{u}\frac{\partial}{\partial x}\right)w'+\frac{1}{\rho_0}\frac{\partial p'}{\partial z}-\frac{\theta'}{\bar{\theta}}g=0$$

$$\frac{\partial u'}{\partial x}+\frac{\partial w'}{\partial z}=0$$

$$\left(\frac{\partial}{\partial t}+\bar{u}\frac{\partial}{\partial x}\right)\theta'+w'\frac{d\bar{\theta}}{dz}=0$$

Linearized Equations

Combine to form a single equation for w'

$$\left(\frac{\partial}{\partial t}+\bar{u}\frac{\partial}{\partial x}\right)^2\left(\frac{\partial^2 w'}{\partial x^2}+\frac{\partial^2 w'}{\partial z^2}\right)+N^2\frac{\partial^2 w'}{\partial x^2}=0$$

N^2 is assumed to be constant.

This has harmonic wave solutions

$$w'=\mathrm{Re}[\hat{w}\exp(i\phi)]=w_r\cos\phi-w_i\sin\phi \tag{7.43}$$

where $\hat{w}=w_r+iw_i$ is a complex amplitude with real part w_r and imaginary part w_i, and $\phi=kx+mz-\nu t$ is the phase, which is assumed to depend linearly on z as well as on x and t. Here the horizontal wave number k is real since the solution is always sinusoidal in x. The vertical wave number $m=m_r+m_i$ may, however, be complex, in which case m_r describes

Solution and Dispersion Relationship

sinusoidal variation in z and m_i describes exponential decay or growth in z depending on whether m_i is positive or negative. When m is real the total wave number may be regarded as a vector $\boldsymbol{\kappa} \equiv (k, m)$, directed perpendicular to lines of constant phase, and in the direction of phase increase, whose components, $k = 2\pi / L_x$ and $m = 2\pi / L_z$, are inversely proportional to the horizontal and vertical wavelengths, respectively. Substitution of the assumed solution into (7.42) yields the dispersion relationship

$$(\nu - \bar{u}k)^2(k^2 + m^2) - N^2 k^2 = 0$$

so that

$$\hat{\nu} \equiv \nu - \bar{u}k = \pm Nk/(k^2 + m^2)^{1/2} = \pm Nk/|\boldsymbol{\kappa}| \qquad (7.44)$$

stopped here 4-12-22

Group Velocity

$$c_{gx} = \frac{\partial \nu}{\partial k} = \bar{u} \pm \frac{Nm^2}{(k^2 + m^2)^{3/2}}$$

$$c_{gz} = \frac{\partial \nu}{\partial m} = \pm \frac{-Nkm}{(k^2 + m^2)^{3/2}}$$

◇ We can show that $\underset{\sim}{c}_g$ is parallel to phase lines:

Let β be angle of $\underset{\sim}{c}_g$ to vertical. Then

$$\cos\beta = \frac{|c_{gz}|}{\left[(c_{gx}-\bar{u})^2 + c_{gz}^2\right]^{1/2}}$$

$$= \frac{k}{(m^2+k^2)^{1/2}}$$

$$= \cos\alpha$$

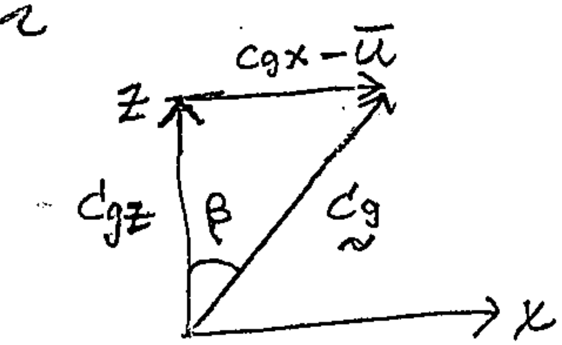

$c_{gx}-\bar{u}$ is flow relative

$k>0$, $m<0$

where α is angle of phase lines to vertical, derived previously.

◇ Group velocity is thus perpendicular to direction of phase propagation.

$$\cos\alpha = \frac{L_x}{(L_x^2+L_z^2)^{1/2}} = \frac{k}{(k^2+m^2)^{1/2}}$$

Solutions for each variable

$$-i\omega\hat{u} + iku_0\hat{u} = -ik\frac{\hat{p}}{\overline{\rho}} \tag{6.48}$$

$$-i\omega\hat{w} + iku_0\hat{w} = -\frac{1}{\overline{\rho}}\frac{\partial\hat{p}}{\partial z} + g\frac{\hat{\theta}}{\overline{\theta}} \tag{6.49}$$

$$ik\hat{u} + \frac{dw}{dz} = 0 \tag{6.50}$$

$$-i\omega\hat{\theta} + iku_0\hat{\theta} + \hat{w}\frac{\mathrm{d}\overline{\theta}}{\mathrm{d}z} = 0. \tag{6.51}$$

Solving for each variable in terms of $\hat{w}$ using (6.37) with $B = 0$, yields

$$\hat{u} = -\frac{m}{k}\hat{w} \tag{6.52}$$

$$\hat{p} = -\frac{\overline{\rho}m(\omega - u_0k)}{k^2}\hat{w} = -\frac{\overline{\rho}m\Omega}{k^2}\hat{w} \tag{6.53}$$

$$\hat{\theta} = -\frac{i}{(\omega - u_0k)}\frac{\mathrm{d}\overline{\theta}}{\mathrm{d}z}\hat{w} = -\frac{i}{\Omega}\frac{\mathrm{d}\overline{\theta}}{\mathrm{d}z}\hat{w}. \tag{6.54}$$

k<0 , m>0: phase lines tilt westward with height

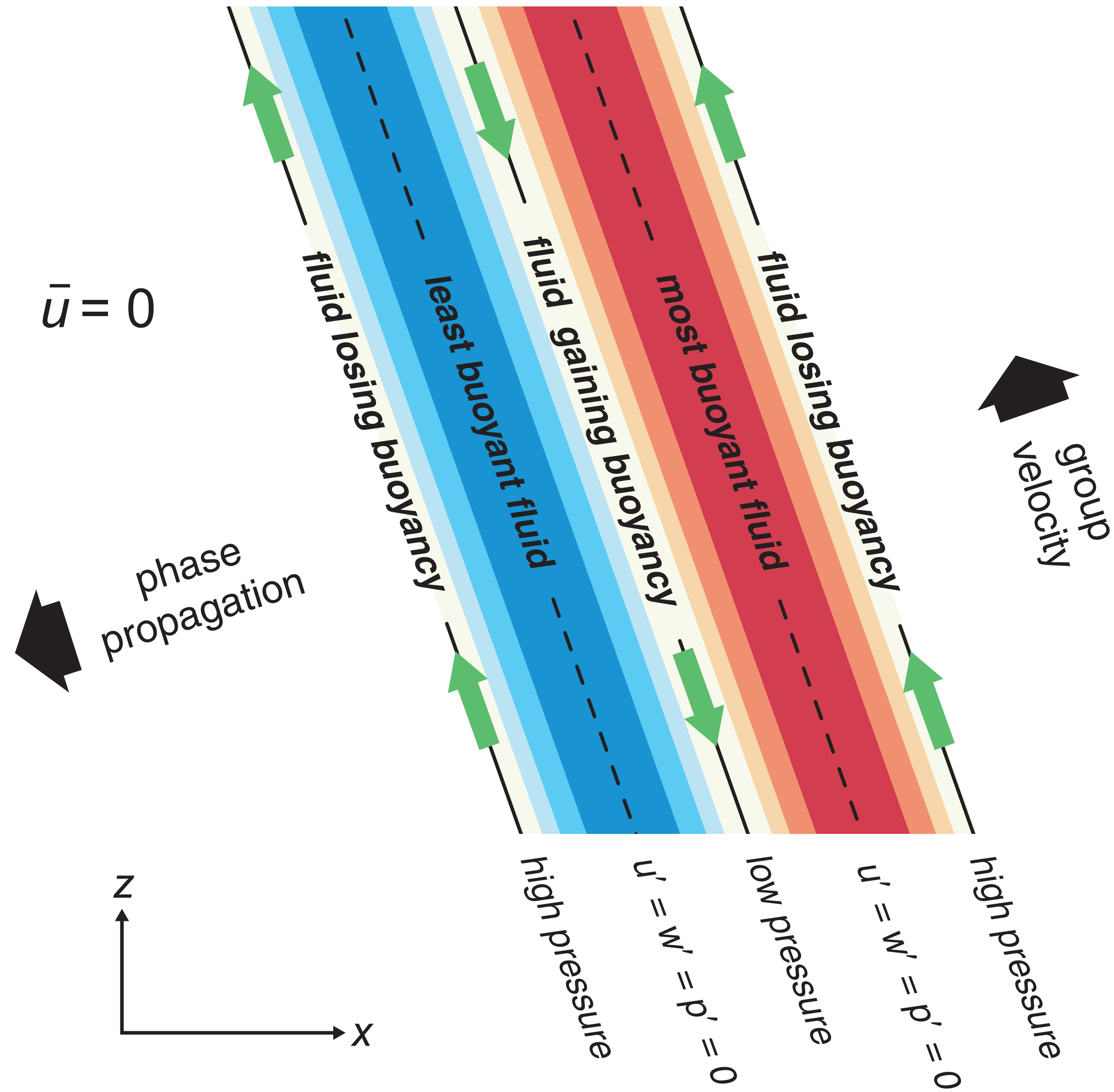

Figure 6.6 Relationship between potential temperature, velocity, and pressure perturbations for an internal gravity wave with $\overline{u} = 0$. (Adapted from Durran [1990].)

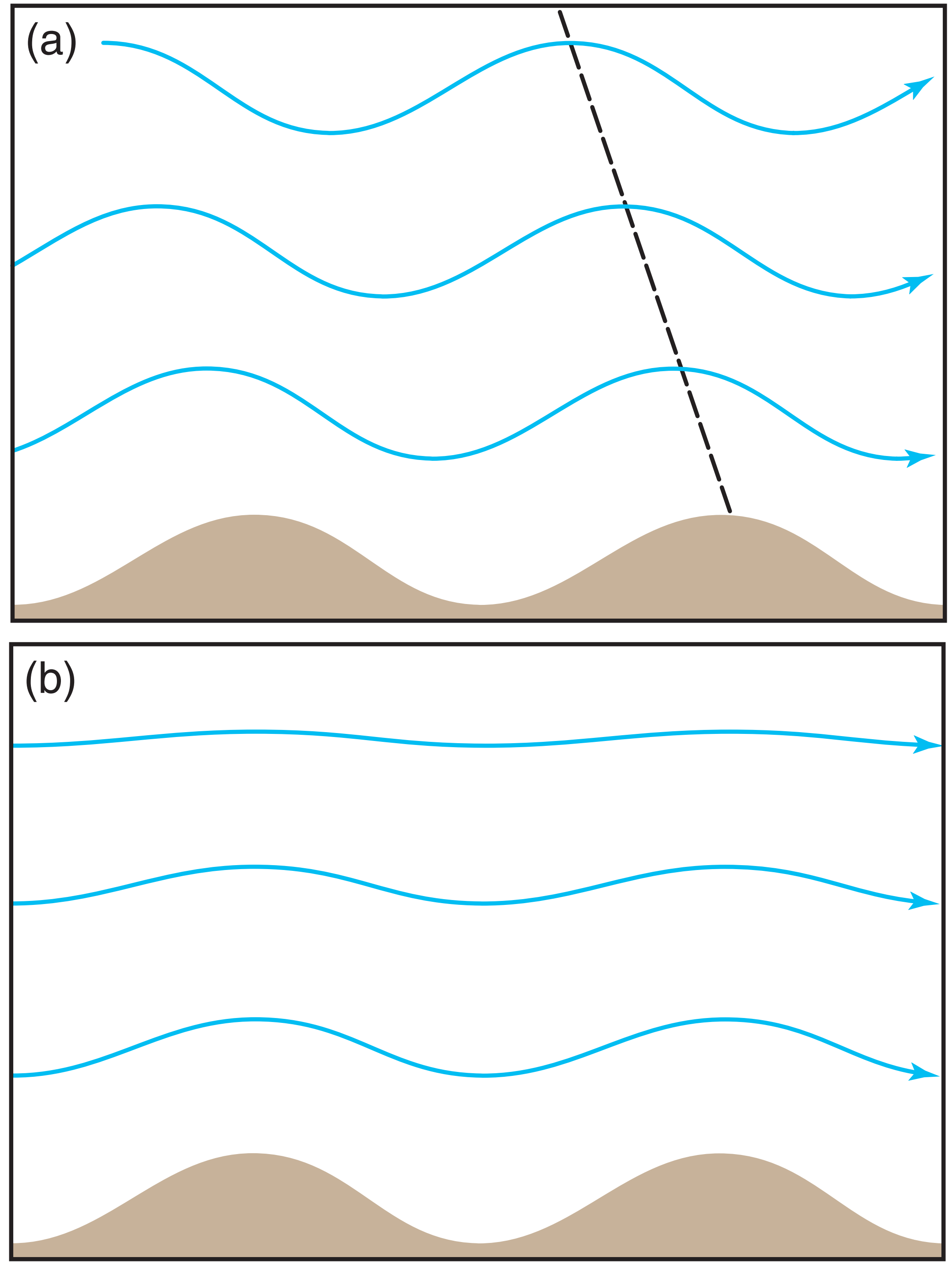

Figure 12.3 Streamlines in steady flow over an infinite series of sinusoidal ridges (a) for the case where $N^2 > u_0^2 k^2$ and (b) for the case where $N^2 < u_0^2 k^2$. The dashed line in (a) shows the phase of maximum upward displacement, which tilts westward with height. (Adapted from Durran [1990].)

Isolated Ridge

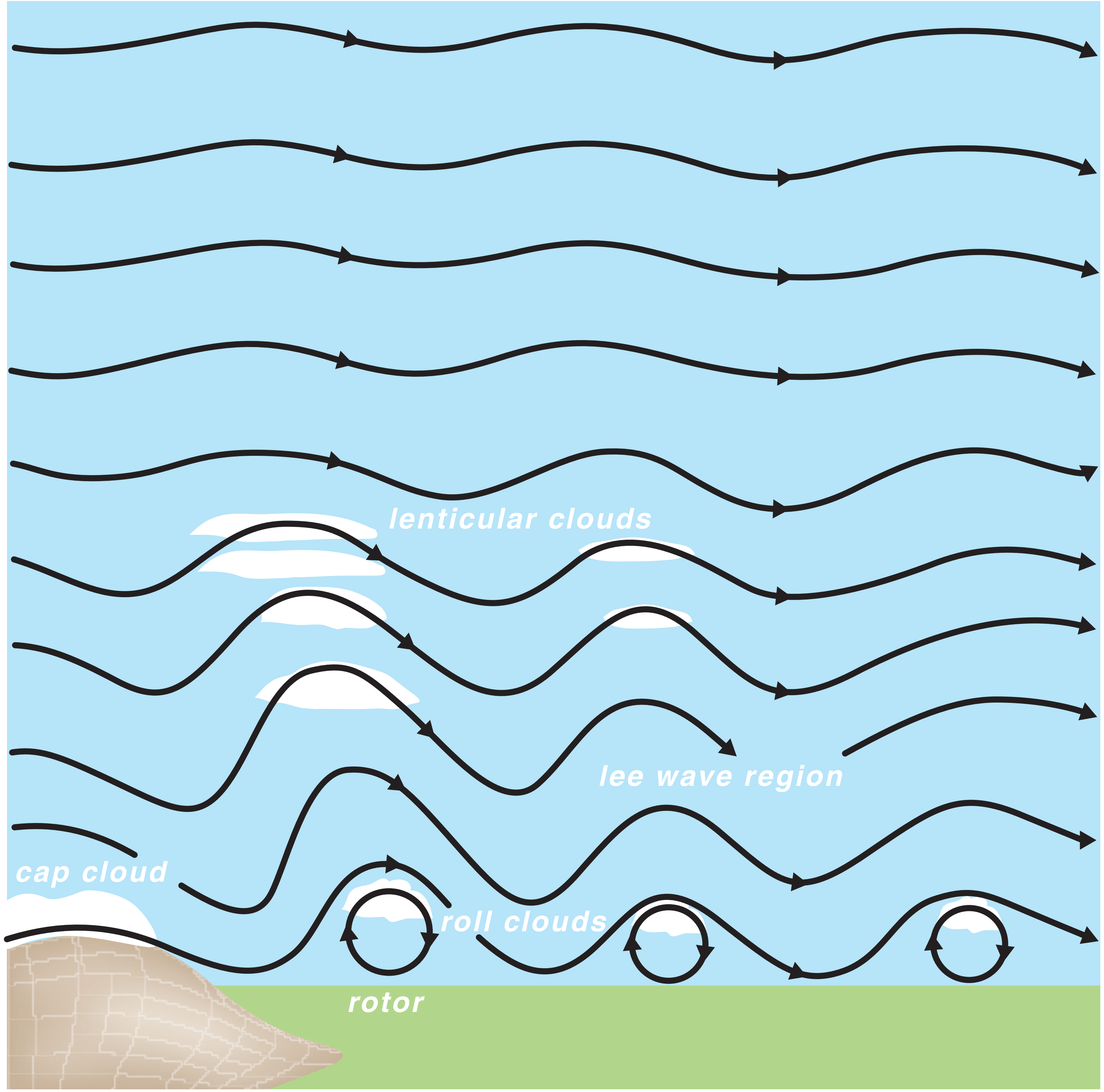

Figure 12.1 Trapped waves and associated clouds in the lee of a mountain ridge. (Adapted from an image provided by the Cooperative Program for Operational Meteorology, Education, and Training [COMET].)

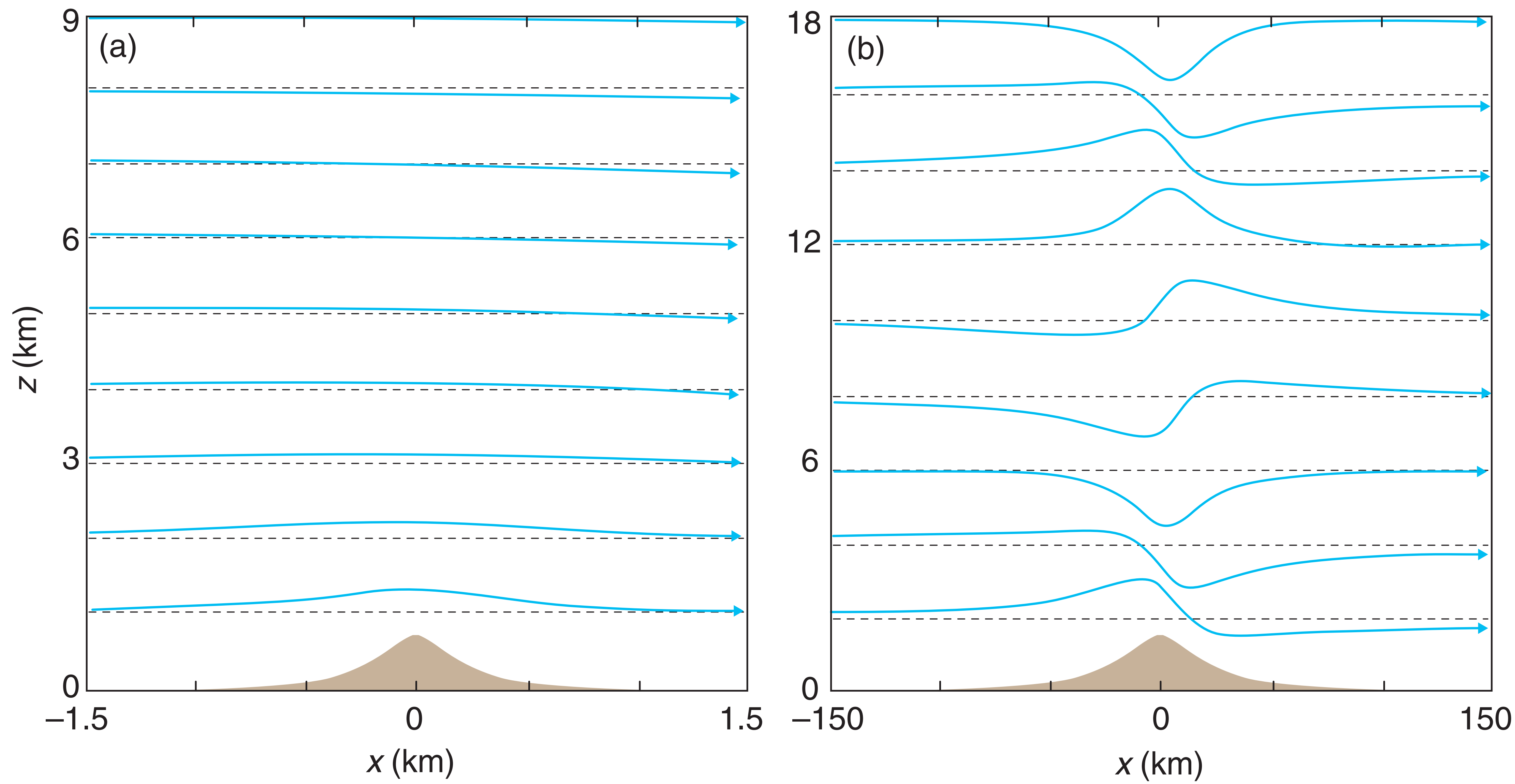

Figure 12.4 Streamlines in steady airflow over an isolated ridge when (a) $u_0 a^{-1} \gg N$ and (b) $u_0 a^{-1} \ll N$. (Adapted from Durran [1986a].)

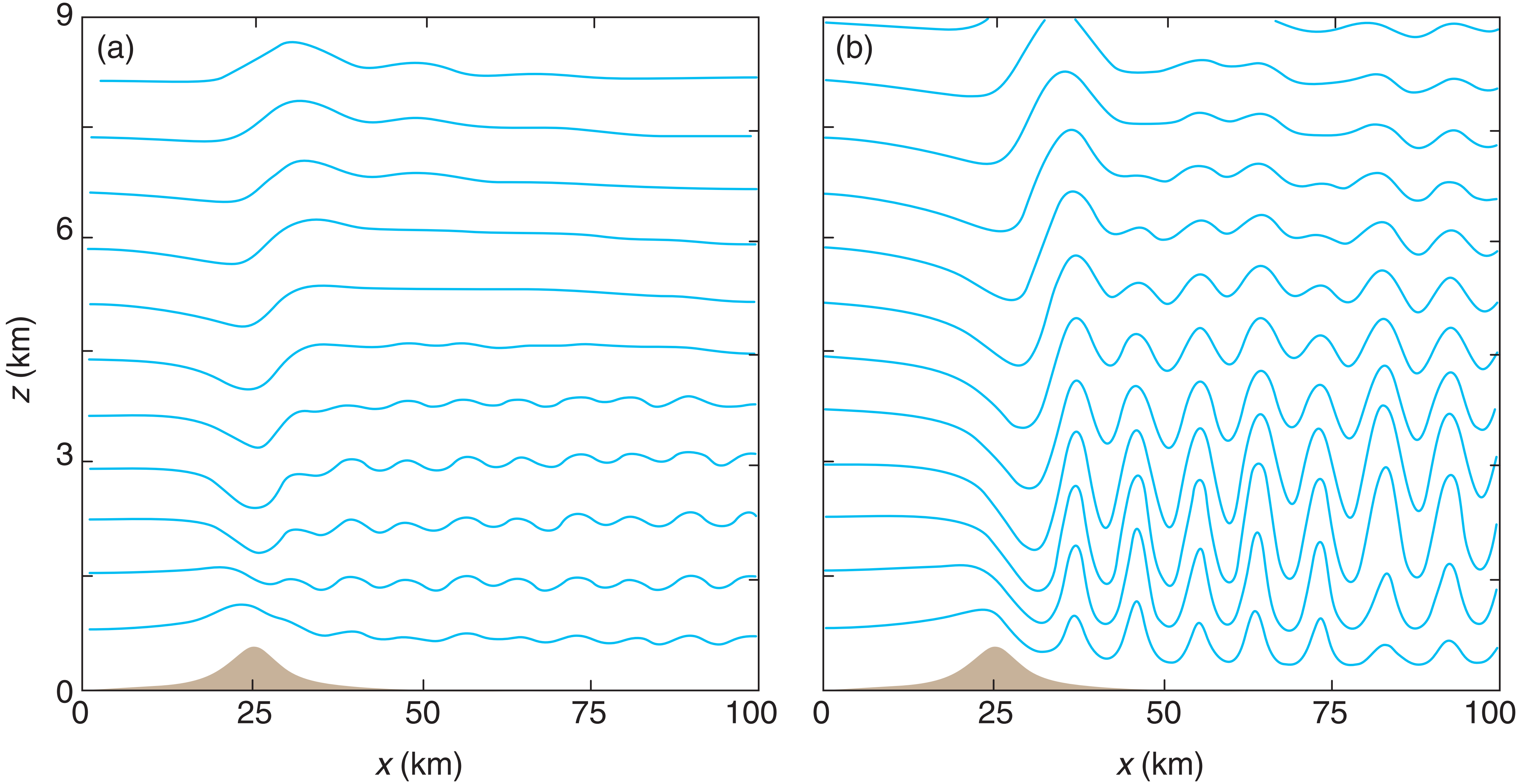

Figure 12.5 Streamlines in air flow over a mountain for (a) steady flow subject to the linear approximation and (b) the fully nonlinear and unsteady solution. (Adapted from Durran [2003a].)

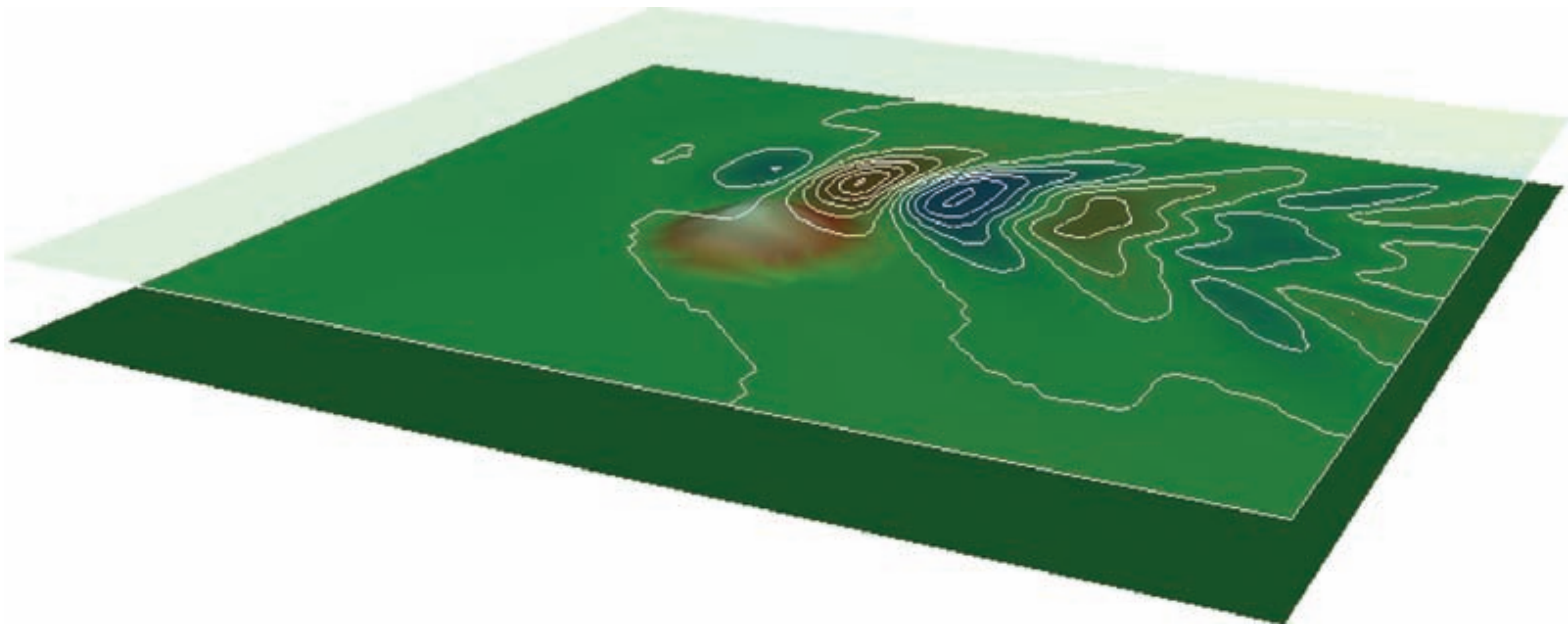

Figure 12.7 Simulation of gravity waves triggered by westerly flow over an isolated peak, as viewed from the southeast. Contours of vertical velocity are shown at an altitude of 6 km at 1 m s^{-1} intervals. Blue (red) shading indicates negative (positive) vertical velocities.

Downslope Windstorms

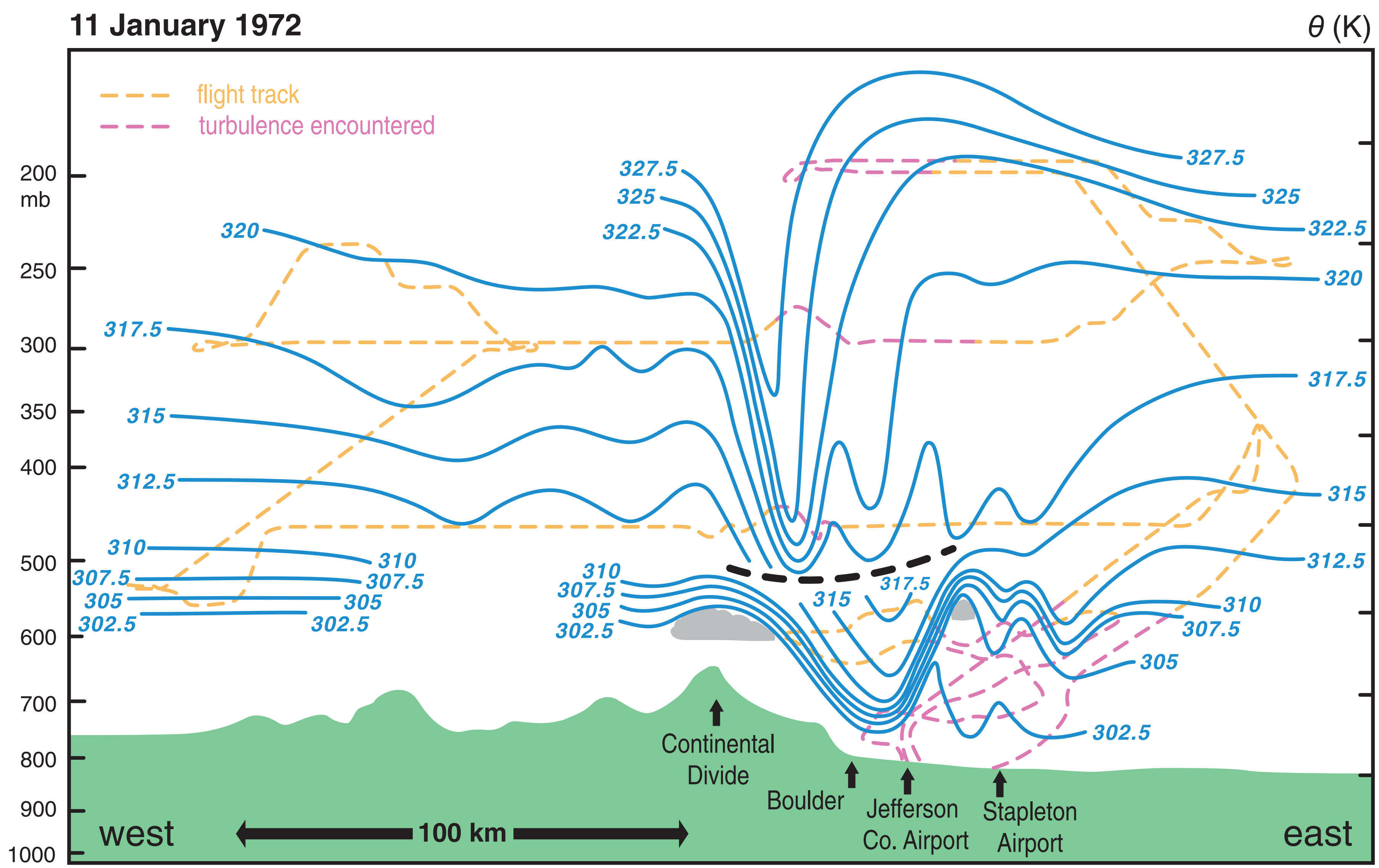

Figure 12.9 Analysis of potential temperatures (blue contours; K) from aircraft flight data (aircraft flight tracks are indicated with dashed lines) and rawinsondes on 11 January 1972 during a downslope windstorm near Boulder, CO. The heavy dashed line separates data taken by the Queen Air at lower levels before 2200 UTC from that taken by the Sabreliner aircraft in the middle and upper troposphere after 0000 GMT (12 January). The aircraft flight tracks were made along an approximate 130°–310° azimuth, but the distances shown are along the east–west projection of these tracks. (Adapted from Lilly [1978].)

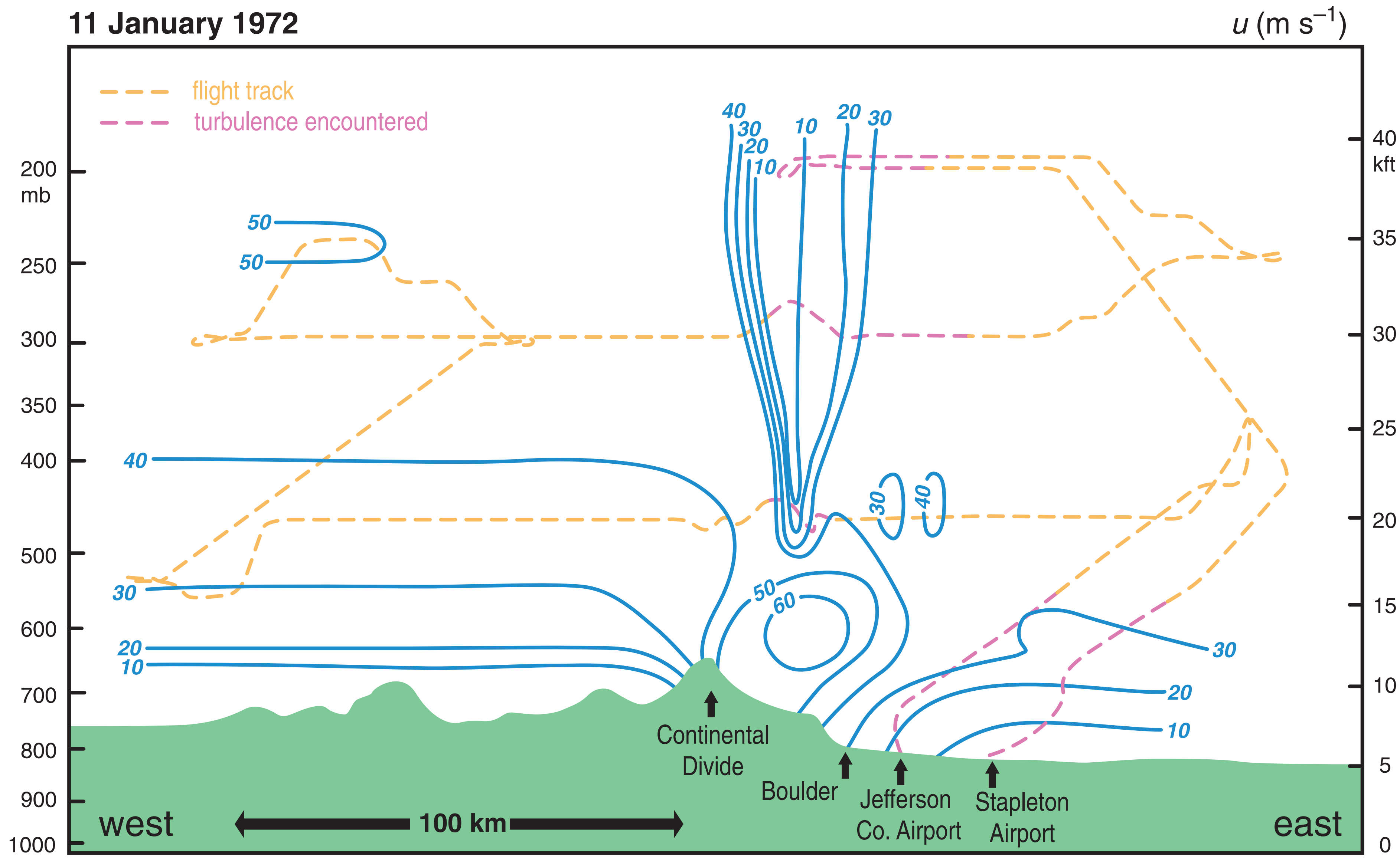

Figure 12.10 Analysis of the westerly wind component (blue contours; m s^{-1}) on 11 January 1972 during the downslope windstorm near Boulder, CO, shown in Figure 12.9. The analysis below 500 mb was partially obtained from vertical integration of the continuity equation, assuming two-dimensional steady-state flow. (Adapted from Klemp and Lilly [1975].)

Shallow Water Model

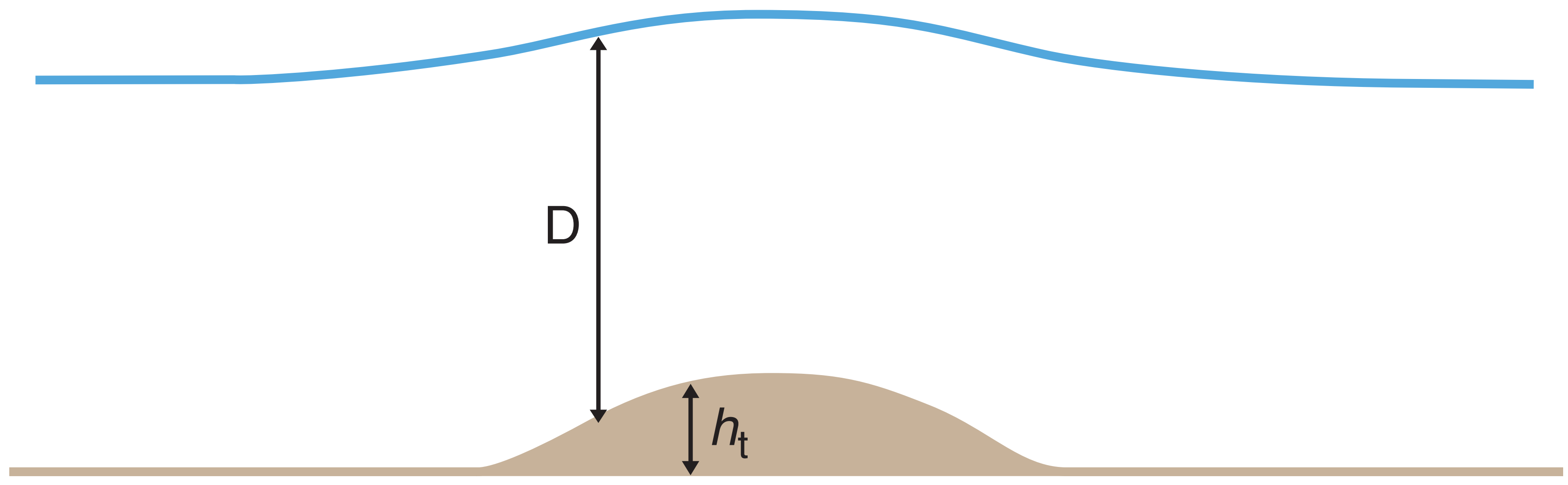

Figure 12.11 Relationship between free surface height, depth (D), and terrain height (h_t).

$$(1 - \mathrm{Fr}^2)\frac{\partial D}{\partial x} = -\frac{\partial h_\mathrm{t}}{\partial x}, \tag{12.26}$$

where $\mathrm{Fr}^2 = u^2/c^2$, and Fr is the *Froude number* for shallow-water theory. The Froude number is the ratio of the mean flow to the gravity wave phase speed. When $\mathrm{Fr} > 1$, gravity waves are unable to propagate upstream relative to the mean flow, and the fluid is unable to produce perturbation pressure gradients of sufficient magnitude to balance nonlinear advection.

The Froude number can be used to identify three distinct flow regimes. Based on inspection of (12.26), if $\mathrm{Fr} > 1$ and $\partial h_\mathrm{t}/\partial x > 0$, then $\partial D/\partial x > 0$ such that the fluid thickens going in the uphill direction, achieving its maximum thickness at the peak of the mountain (Figure 12.12a). On the lee slope, where $\partial h_\mathrm{t}/\partial x < 0$, the fluid thins. As the thickness of the fluid changes, the zonal velocity also changes in accordance with the constant zonal mass flux prescribed

In contrast, when $\mathrm{Fr} < 1$, termed *subcritical flow*, (12.26) predicts that the fluid will thin ($\partial h_{\mathrm{t}}/\partial x < 0$) as the terrain height increases ($\partial h_{\mathrm{t}}/\partial x > 0$) (Figure 12.12b). Accompanying this thinning is an increase in the zonal wind speed, reaching a maximum value at the top of the mountain where the fluid is thinnest. The behavior associated with subcritical flow as a parcel traverses a mountain is not in line with our usual arguments regarding the simple transfer of energy from kinetic to potential, and we must break with our conceptual model of an isolated ball rolling up a hill. An individual air parcel is not isolated the leeward side occur for supercritical flow. Thus, to achieve acceleration along the entire path, the flow must undergo a transition from subcritical on the windward side to supercritical as it crests the mountain. In other words, the acceleration on the windward side must cause u to cross the threshold from subcritical to supercritical flow, which is likely to happen only if the flow has a Fr close to unity at the start. The transition from subcritical to supercritical results in leeward wind speeds that exceed their original value on the windward side. In accordance with the increasing speeds, the fluid thickness will decrease over the entire path, causing the free surface to drop sharply on the leeward side, analogous to the descending isentropes during downslope wind events, and resulting in what is called a *hydraulic jump*. Hydraulic jumps are very turbulent, and large amounts of energy are dissipated within them.[6]

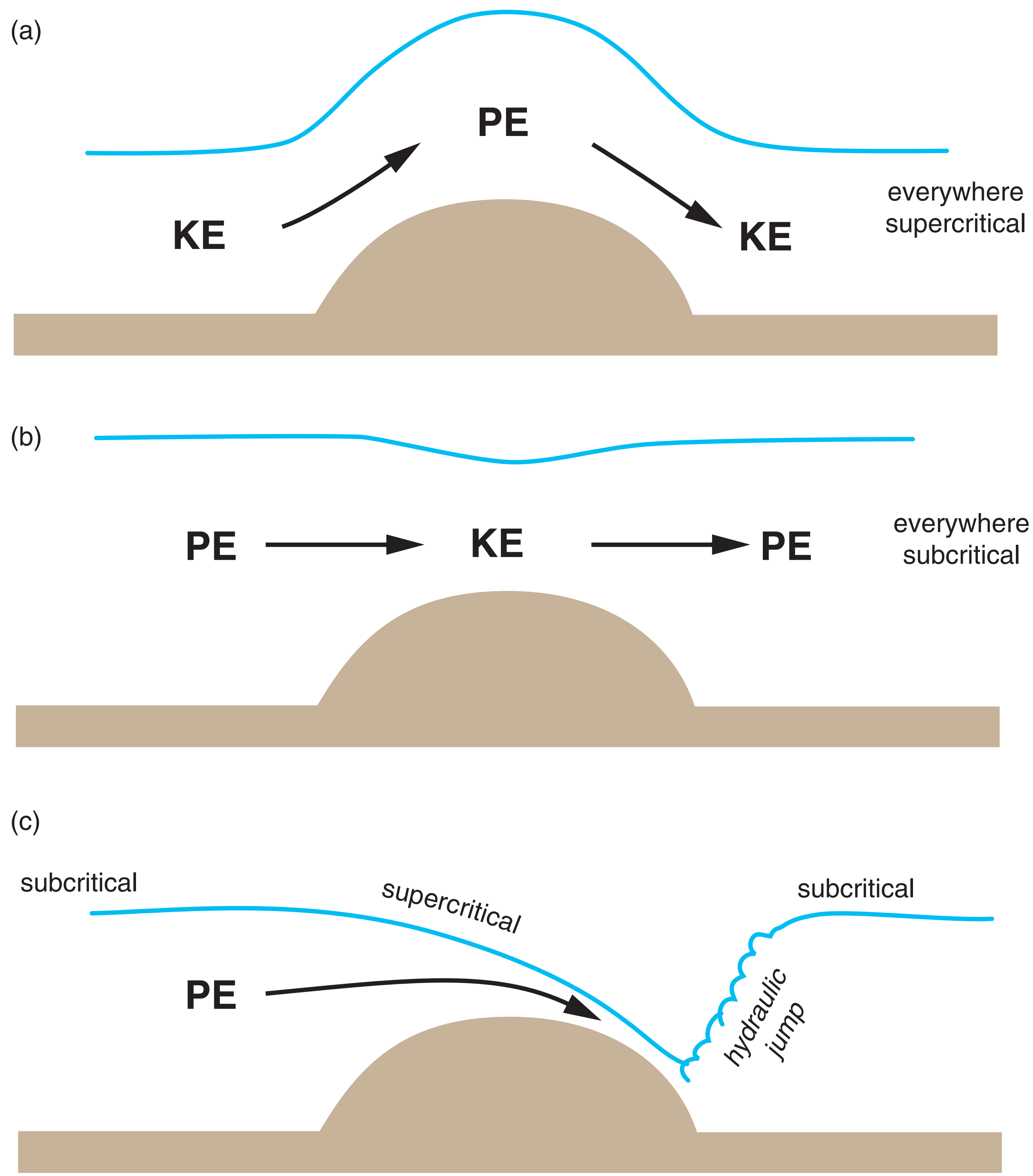

Figure 12.12 Flow over an obstacle for the simple case of a single layer of fluid having a free surface. (a) Supercritical flow ($Fr > 1$) everywhere. (b) Subcritical flow ($Fr < 1$) everywhere. (c) Supercritical flow on the lee slope with adjustment to subcritical flow at a hydraulic jump near the base of the obstacle. (From Durran [1990].)

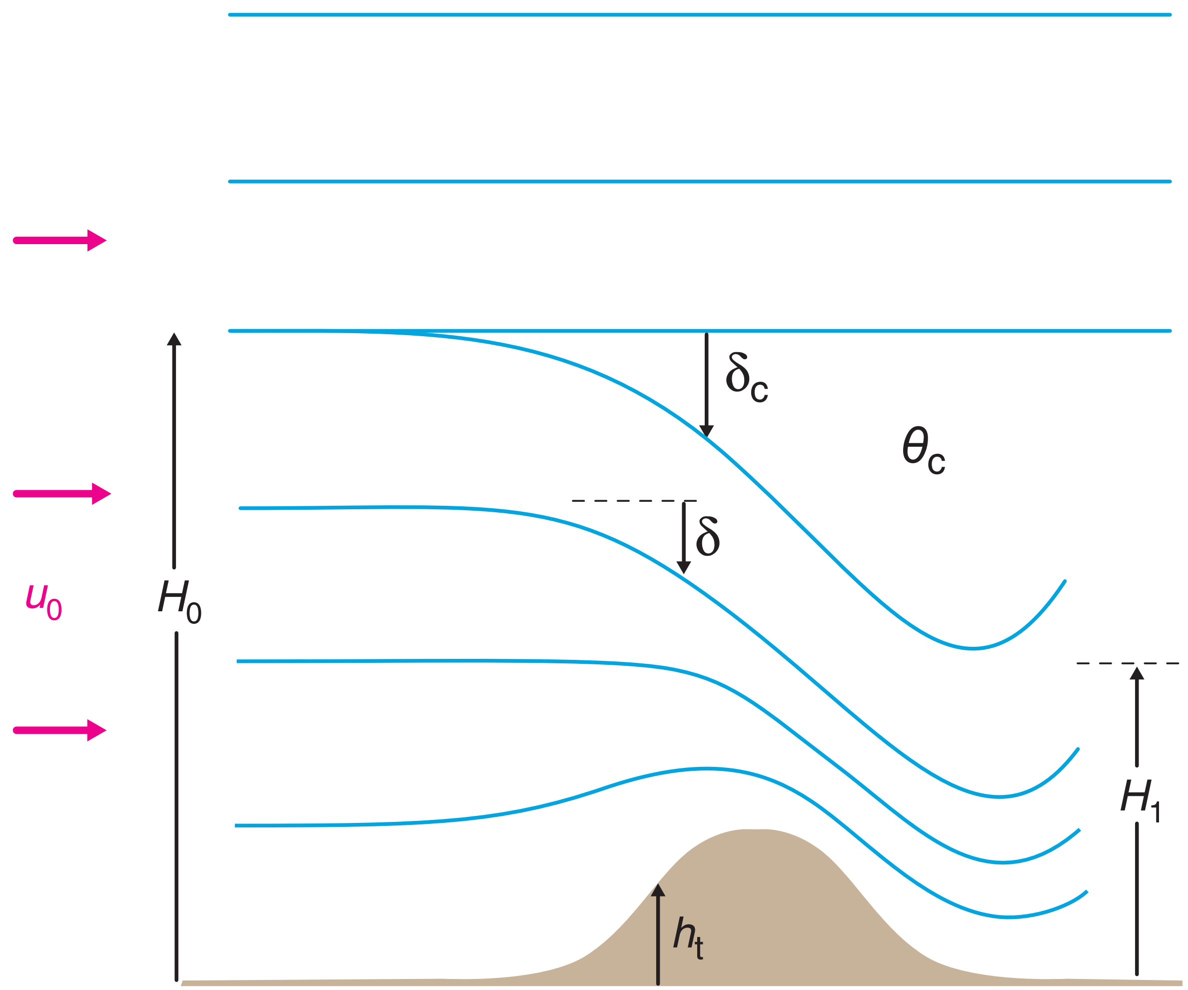

Figure 12.13 Schematic of the idealized high-wind-speed flow configuration, derived from aircraft observations and numerical simulations. A certain critical streamline divides and encompasses a region of uniform potential temperature. H_0 is the original height of the dividing streamline, θ_c is the potential temperature in the well-mixed region between the split streamlines, δ is the displacement of an arbitrary streamline, δ_c is the displacement of the dividing streamline, and H_1 is the nadir of the lower dividing streamline. (From Smith [1985].)

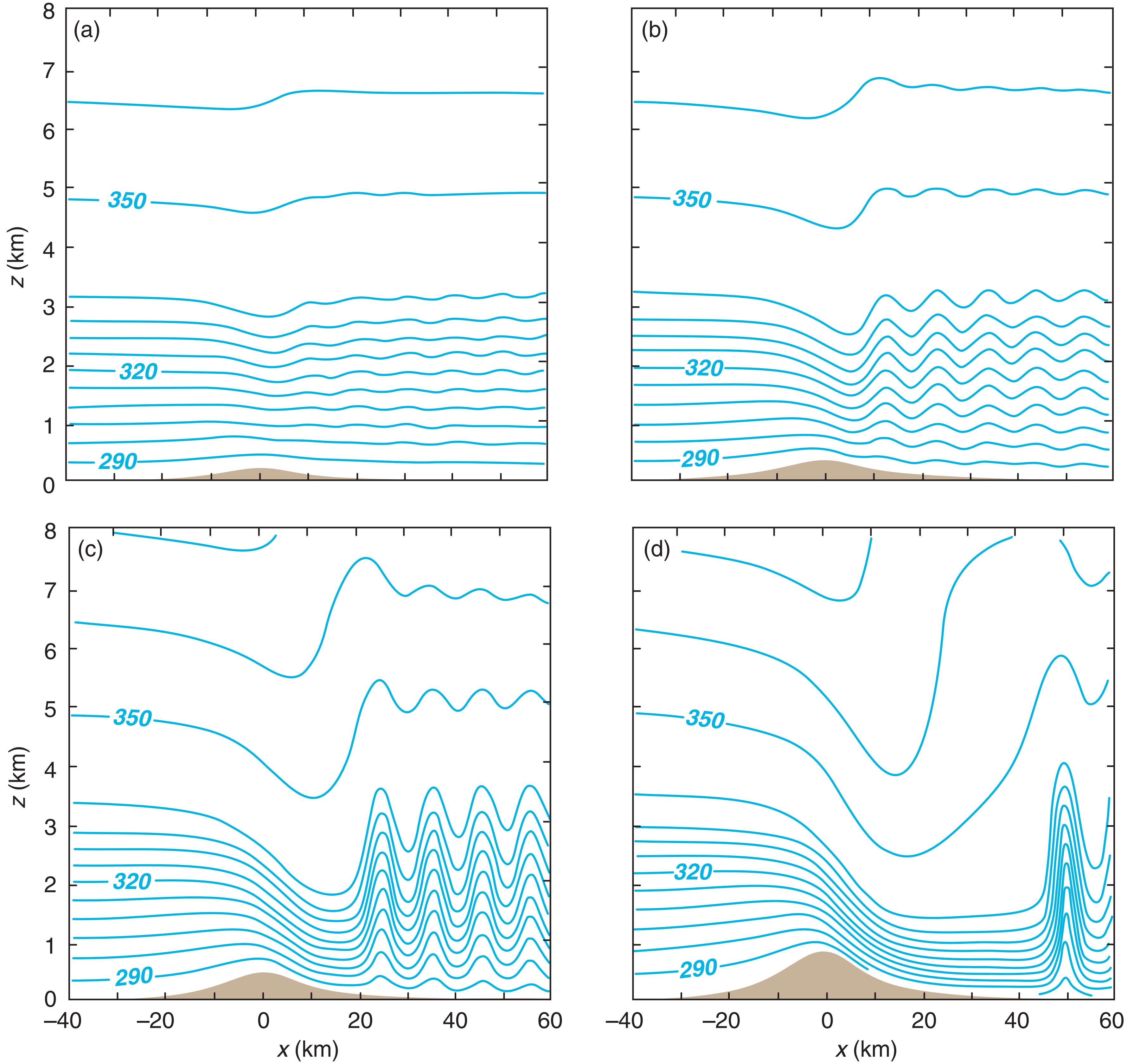

Figure 12.14 Isentropes for the airflow in a two-layer atmosphere when the interface is fixed at 3000 m, and the mountain height is (a) 200, (b) 300, (c) 500, and (d) 800 m. (From Durran [1986b].)

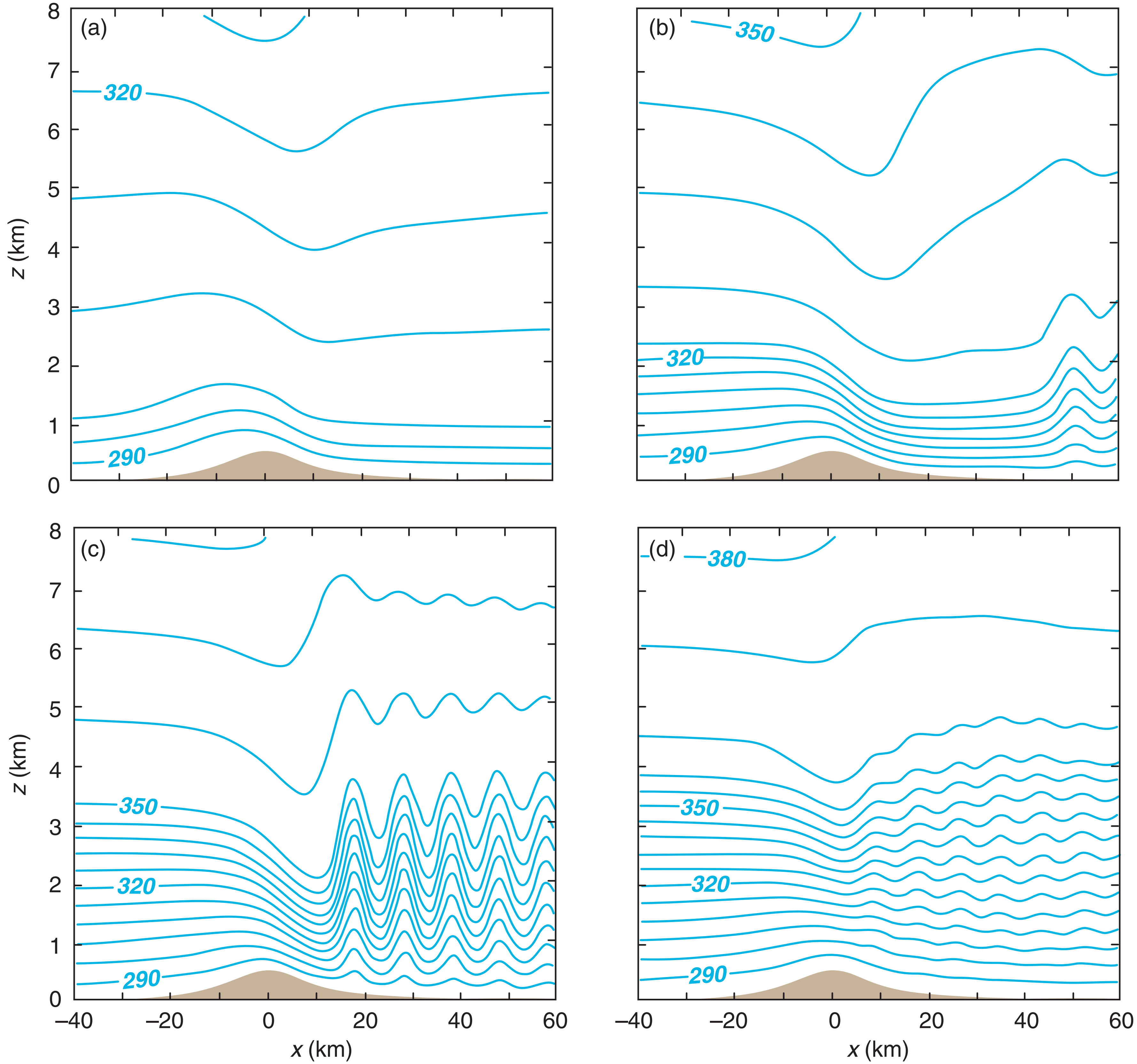

Figure 12.15 Isentropes for the airflow in a two-layer atmosphere when the mountain height is fixed at 500 m, and the interface is at (a) 1000 m, (b) 2500 m, (c) 3500 m, and (d) 4000 m. (From Durran [1986b].)

Putting all of this together, here are some of the conditions that forecasters look for when predicting downslope windstorms:

- an asymmetric mountain with a gentle windward slope and a steep lee slope
- strong cross-mountain geostrophic winds ($>15\,\mathrm{m\ s^{-1}}$) at and just above mountain-top level associated with surface high pressure upstream and surface low pressure downstream
- an angle between the cross-mountain flow and the ridge that is greater than $\sim 60^\circ$
- a stable layer near or just above the mountain top, and a layer of lesser stability above
- a level that exhibits a wind direction reversal or where the cross-barrier flow simply goes to zero (the mean state critical level); the existence of weak, vertical wind shear or reverse shear is more favorable than forward shear
- situations of cold advection and anticyclonic vorticity advection, which promote downward synoptic motion to generate and reinforce the vertical stability structure
- absence of a deep, cold, stable layer in the lee of mountains, which may keep the downslope flow from penetrating to the surface.